Experimental Analysis of 5G Candidate Waveforms and their Coexistence with 4G Systems

Florian Kaltenberger and Raymond Knopp
EURECOM
Sophia-Antipolis, France

Carmine Vitiello
University of Pisa
Pisa, Italy

Martin Danneberg and Andreas Festag
Vodafone Chair Mobile Communication Systems
Technische Universität Dresden, Germany

Abstract—The 5G mobile standard will very likely include a new waveform that addresses scenarios like sporadic low-latency traffic and dynamic spectrum access (DSA). In both cases the current 4G waveforms have some deficiencies, like the need for strict synchronicity and the high adjacent channel leakage ratio (ACLR) respectively. Several candidate waveforms can be found in the literature, such Generalized Frequency Division Multiplexing (GFDM), and Universal Filtered Multi-Carrier (UFMC). Both use a digital multi-carrier transceiver concept that employs pulse shaping filters to provide control over the transmitted signal's spectral properties. In this paper we will present experimental results that evaluate the impact of these two waveforms on an existing 4G system. The 4G system was based on Eurecom's OpenAirInterface for the eNB and a commercial UE. The new waveform was generated using a signal generator.

I. INTRODUCTION

LTE-Advanced is a fourth generation (4G) mobile system that is currently being deployed worldwide. In the meantime, researchers are already thinking about a fifth generation mobile system, referred to as 5G, that should provide 1000 times more capacity and less latency than 4G systems, support for an unprecedented number of users and connected things, and ensure better energy efficiency [1]. From a physical layer (PHY) point of view, these requirements translate into higher spectral efficiency, the ability to support large and fragmented spectrum, dynamic spectrum access (DSA), and short packet transmissions with loose synchronization requirements. Orthogonal frequency division multiplexing (OFDM) and single-carrier frequency division multiplexing (SC-FDMA), which are the two waveforms used in current 4G systems do not fulfill all of these requirements, and therefore new waveforms have been proposed for 5G.

All proposed candidate 5G waveforms are generalizations of OFDM. In case of filter-bank multi-carrier (FBMC) additional pulse-shaping filters are applied to every subcarriers [2]. Alternatively, universal filtered multi-carrier (UFMC) [3] applies filtering over multiple subcarriers, and generalized frequency division multiplexing (GFDM) [4] uses circular convolution instead of linear convolution for the filtering of the subcarriers. All of these waveforms have in common that they reduce the adjacent channel leakage ratio (ACLR) and the peak-to-average power ratio (PAPR) compared to an OFDM system at the expense of a more complex receiver design.

This paper is an extension of [5], where have shown a comparative study of GFDM, SC-FDMA, and OFDM in a cognitive radio setting. We showed that GFDM can be used with about 5 dB higher transmit power than a corresponding
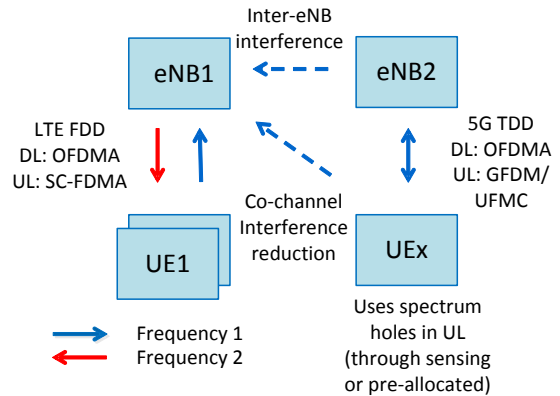

Fig. 1. Dynamic spectrum access application scenario. The primary system operates in FDD, while the secondary system operates in TDD using the UL frequency of the primary system. The inter-eNB interference can be neglected if the second eNB is sufficiently far away or indoors (typical macro/small cell HetNet scenario).

orthogonal frequency division multiplexing (OFDM) system, before any impact on the primary system is noticeable. The results from our real-time measurements were validated by simulations. In this paper we extend this work by including the UFMC waveform in the comparison.

In our scenario, the primary system is a 4G LTE FDD system and the secondary system is a 5G TDD system that operates in the uplink frequency band of the primary system and exploits spectrum holes of a primary system. We experimentally study the performance of the primary system in presence of interference from the secondary system, which is using either UFDM, GFDM, SC-FDMA, or OFDM. The 4G system is based on Eurecom's OpenAirInterface [6] for the eNB and a commercial UE. The 5G waveforms are generated offline and transmitted using a signal generator.

II. APPLICATION SCENARIO

The application scenario is depicted in Figure 1. The primary system (denoted by eNB1 and UE1) is a 4G LTE FDD system using OFDMA in the downlink and SC-FDMA in the uplink. The secondary system (denoted by eNB2 and UEx) is a 5G TDD system that operates in the uplink band of the primary system, exploiting spectrum holes in the primary system in order not to create any interference on the uplink to the primary eNB1. The interference on the downlink of the secondary system, i.e., from eNB2 to eNB1 can be neglected
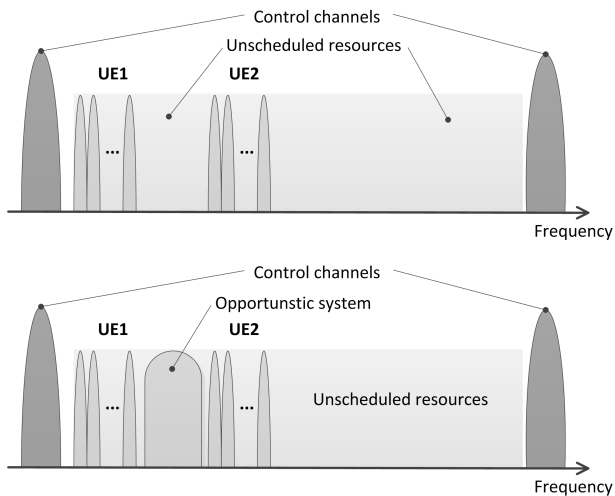
Fig. 2. Spectrum of the uplink showing the primary system and a secondary system that exploits spectrum holes.

if the second eNB is sufficiently far away or indoors (typical macro/small cell HetNet scenario), which we assume here.

In Figure 2 we show a schematic of the UL spectrum showing both the primary and the secondary system. In LTE the first and the last physical resource block (PRB) of the UL are reserved for control channels. The rest of the resources can be dynamically allocated to different UEs by the eNB scheduler. If the cell is not fully loaded it implies that some UL resources remain unscheduled and can thus be potentially used by the secondary system. The method to detect the spectrum holes is out of the scope of this paper and the reader is referred to the literature [7]. In this work we program the eNB such that it is always leaves a predefined set of resource blocks unscheduled.

III. GFDM AND UFMC

Both GFDM and UFMC were implemented and parameterized to fit the sampling and framing of the LTE standard. In this work we focus on the case of 10MHz channelization, which is usually implemented using a sampling rate of 15.35Msps and a DFT size of $N = 1024$.

A. UFMC

The classical architecture of the UFMC transmitter [3] is depicted in Figure 3. It uses a 1024-IDFT and a Dolph-Chebyshev filter per each branch, both shifted to the center of the respective subband. The filter length L has been fixed to the same length of OFDM cyclic prefix plus one (73 or 81), in order to maintain the same output length at the end of the convolution operation. DFT operation is optionally and it can be used in case of SC-UFMC with comparing to SC-FDMA. Its dimension is fixed to $12B$, where B is the number of PRBs and 12 is the number of subcarriers per PRB.

If only a few (e.g., 1–3) PRBs shall be generated (which is the case of interest here), some optimizations with respect to [3] can be applied. The classical scheme doesn't show good computational performance because a 1024-IDFT operation
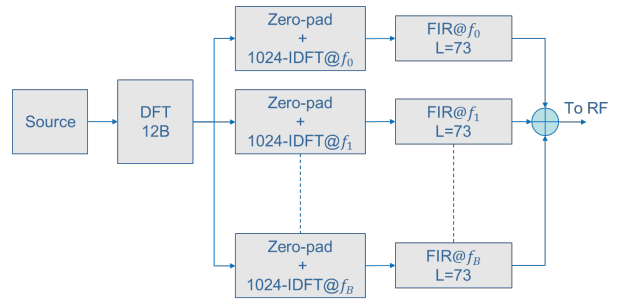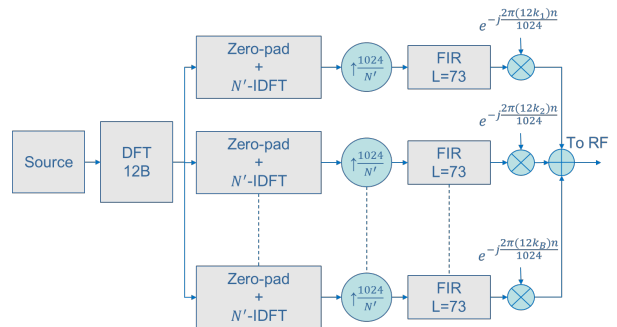

Fig. 3. Classical UFMC transmitter scheme [3].

Fig. 4. Modified UFMC transmitter scheme.

is performed over 12, 24 o 36 complex samples and producing 1024 complex samples that will be filtered entirely. Furthermore using a shifted version of the filter, convolution operation is performed using complex filter taps, redoubling the amount of operations. For simplifying transmitter scheme, we decreased the IDFT dimension using a correct upsampling and move frequency shift operation to the end of transmission chain as depicted in Figure 4.

The IDFT dimension, which is indicated with N', represents the heart of our computational complexity reduction process, because a value too small leads to have an high upsampling factor thus overlapping of replicated signals in frequency domain, while a value too high leads to have a small upsampling rate wasting useful computational resources. For the transmission of only one PRB, we show the UFMC spectrum (blue) shape in comparison with an OFDM spectrum (red) for different values of N' in Figure 5. Using 16-IDFT dimension and upsampling factor of 64, we can find spurious repetitions within filter bandwidth that create heavy out-of-band (OOB) emissions and therefore the quality of our signal is not good. Employing 32-IDFT and upsampling factor of 32, we can find contributions of spurious repetition at the edges of filter bandwidth and it damages the spectrum in terms of OOB emission because they are not attenuated enough (around -30dB). Using 64-IDFT and upsampling factor of 16, finally we have not in-band spurious repetition and only one contribute at -60db out of band, much lower than OFDM OOB emission. Comparing 64-IDFT with 1024-IDFT, we can note that the spectrums have more or less the same shape and features but saving a lot of computational resources on IDFT operation and filtering. For this reason we use $N' = \min(64, 2^{\lceil \log_2 12B \rceil})$ improving computational performance of our scheme without losing spectrum features.
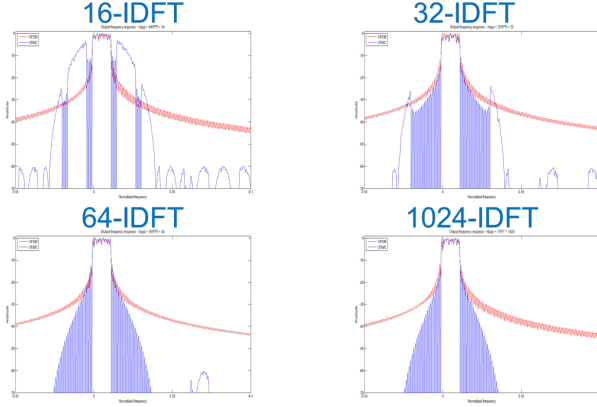
Fig. 5. UFMC spectrum(blue) at varying of IDFT dimension comparing with OFDM spectrum(red).
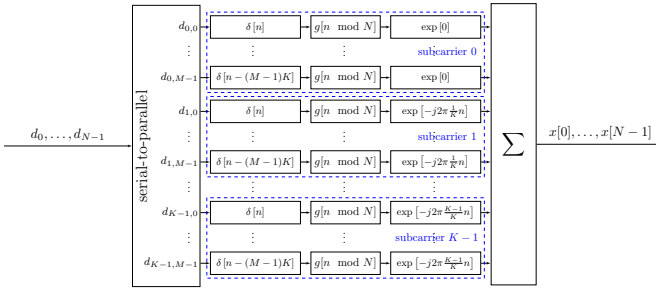

Fig. 6. GFDM transmitter system model as depicted in [4].

B. GFDM

GFDM is a multicarrier system with flexible pulse shaping. In this section, the GFDM transmitter is briefly described as a basis for the experimental work in the next section. A detailed description of the GFDM transmitter and receiver can be found in [4].

The GFDM transmitter structure is presented in Figure 6. At the input, the binary data is split up into blocks of KM complex valued data symbols, where K is the number of subcarriers and M the subsymbols. Each such GFDM data block $d_{k,m}$ is first up sampled by the factor N/K, such that the circular pulse shaping filter g can be applied. Afterwards the pulse shaped symbol is up converted by $e^{j2\pi\frac{k}{K}n}$ to the kth subcarrier.

Each GFDM subsymbol occupies N samples and multiple subsymbols are grouped into a GFDM block. A cyclic prefix (CP) is added for an entire GFDM block, which increases spectral efficiency compared to classical OFDM or SC-FDMA. Guard symbols can be inserted at the start and the end of the block to reduce OOB emissions, at the cost of spectral efficiency.

To make GFDM compatible to the LTE framing and comparable to the UFMC implementation, we set the number of used subcarriers to $K = 12B$ and the number of subsymbols to $M = 12$ plus one subsymbol for the cyclic prefix. Further we add two guard symbols to reduce OOB emissions. These guard symbols can potentially be used for pilots [4]. As a filter we apply a raised cosine filter with a roll-off factor of 0.
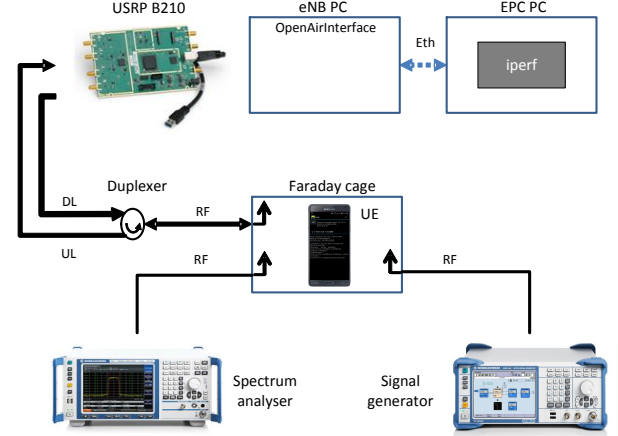

Fig. 7. Experimental setup.

IV. EXPERIMENTAL SETUP

The experimental setup is depicted in Figure 7. The eNB of the primary system is implemented using the OpenAirInterface eNB, which consists of an off-the-shelf PC running the OpenAir4G LTE Rel 8 software modem and an USRP B210 radio card. The eNB is connected via Ethernet to another PC running the evolved packet core (EPC). The UE is a Samsung Galaxy Note 4. This setup allows for an end-to-end application layer connection between the Smartphone and the internet. We use the *iperf* application to measure the throughput between the UE and the EPC.

The secondary UE is emulated using a SMBV signal generator from Rhode&Schwarz. The GFDM waveforms is generated in Matlab while the UFMC waveform is generated by the UL simulator of the OpenAirInterface software.

The antenna of the primary eNB as well as the UE are placed inside a Faraday cage to guarantee that we are not receiving any other interference and also that we are not creating any harmful interference to commercial LTE networks. Finally the signal generator and a spectrum analyzer are also connected to antennas in the Faraday cage and allows us to observe both the primary and the secondary system at the same time.

The primary eNB has been configured in LTE band 7 (FDD) with a DL carrier frequency of 2.68 GHz, a transmission bandwidth of 10 MHz (50 PRBs), transmission mode 1 (SISO), and a total output power of 0 dBm. The scheduler of the eNB has been configured in such a way that it only schedules RBs 1–20 on the UL. Further the UL modulation and coding scheme (MCS) has been set to 16, which corresponds to 16QAM modulation, and a transport block size (TBS) of 6200 bits per subframe. Since we only schedule 4 subframes out of the available 10, the total PHY layer throughput 2.48 Mbps. Due to protocol overhead from layer 2 and layer 3, the maximum throughput at the application layer is slightly less.

The secondary system is using either an OFDM, SC-FDMA, GFDM, or UFMC waveform. They are all configured such that they occupy PRBs 21–23, such that they do not overlap with the primary system. It should be noted that for the SC-FDMA waveform we have removed the 7.5kHz offset
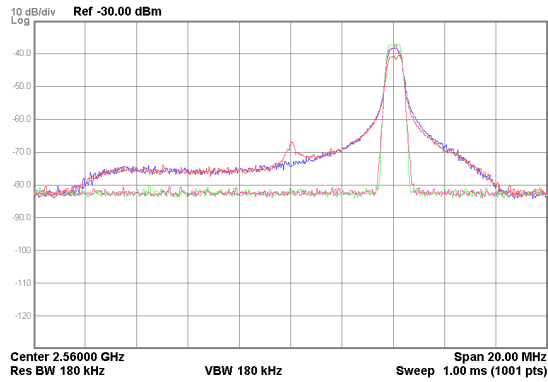
Fig. 8. Screenshot of the spectrum analyzer comparing the spectra of the different waveforms.

Fig. 9. UL goodput of the primary system as a function of the secondary TX power.

that is usually applied in the standard in order to make align it with the other waveforms.

A. The OpenAirInterface Platform

OpenAirInterface[1] (OAI) is an open-source hardware/software development platform and an open forum for innovation in the area of digital radio communications. OpenAirInterface software modem comprises a highly optimized C implementation of all the elements of the 3GPP LTE Rel 8 protocol stack plus some elements from Rel 10 for both user equipment (UE) and enhanced node B (eNB). The software modem can be run in simulation/emulation mode or in real-time mode together with a hardware target. EURECOM has developed its own hardware target, called ExpressMIMO2, which supports up to four antennas and a bandwidth of up to 20MHz and a frequency range from 300MHz to 3.8GHz. Recently, OAI has also been ported to run on universal software radio peripheral (USRP) B210 platform from *Ettus Research*, a *National Instrument* (NI) company.

The current software modem can interoperate with commercial LTE terminals and can be interconnected with closed-source EPC (enhanced packet core) solutions from third-parties. Recently an open-source implementation of the EPC has also been developed at EURECOM and is now part of the Openair4G software suite. The objective of this platform is to provide methods for protocol validation, performance evaluation and pre-deployment system test. See [6] for more details.

V. RESULTS

First we compare the spectra of the different waveforms in in Figure 8. It can be seen that OFDM and SC-FDMA both have rather large OOB emissions while GFDM and UFMC have rather steep spectral masks.

In the experimental setup we measure the goodput of the primary system after the UE has successfully connected to the eNB. To this end we use the *iperf* application to generate UDP traffic at the UE at a rate of 2.48 Mbps for 10 seconds. The goodput is recorded at the eNB also with the *iperf* application.
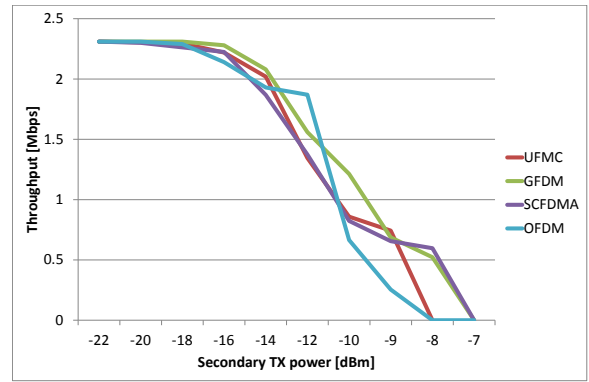
In Figure 9 we show the results as a function of the secondary TX power. Unfortunately the results are not very conclusive, but it can be seen that UFMC and GFDM do perform better than SC-FDMA.

VI. CONCLUSION

We have shown through real-time experiments the benefits of UFMC and GFDM over OFDM and SC-FDMA in a cognitive radio setting, where UFMC and GFDM are used as a waveform for a secondary system that opportunistically exploits spectrum holes in a primary LTE system. Both UFMC and GFDM have a much lower adjacent channel leakage ratio, even when it operates without time or frequency synchronization to the primary system. Experiments were carried out using Eurecom's OpenAirInterface and a commercial UE as a primary system and a signal generator transmitting the secondary waveform. Future work includes the integration of UFMC transmitter and receiver into OpenAirInterface as well as a more in-depth performance analysis between GFDM and UFMC.

REFERENCES

[1] J. Andrews, S. Buzzi, W. Choi, S. Hanly, A. Lozano, A. Soong, and J. Zhang, "What Will 5G Be?" *Selected Areas in Communications, IEEE Journal on*, vol. 32, no. 6, pp. 1065–1082, June 2014.

[2] B. Farhang-Boroujeny, "OFDM Versus Filter Bank Multicarrier," *Signal Processing Magazine, IEEE*, vol. 28, no. 3, pp. 92–112, May 2011.

[3] G. Wunder et al., "5GNOW: Non-orthogonal, Asynchronous Waveforms for Future Mobile Applications," *Communications Magazine, IEEE*, vol. 52, no. 2, pp. 97–105, February 2014.

[4] N. Michailow, M. Matthe, I. Gaspar, A. Caldevilla, L. Mendes, A. Festag, and G. Fettweis, "Generalized Frequency Division Multiplexing for 5th Generation Cellular Networks," *Communications, IEEE Transactions on*, vol. 62, no. 9, pp. 3045–3061, Sept 2014.

[5] F. Kaltenberger, R. Knopp, M. Danneberg, and A. Festag, "Experimental analysis and simulative validation of dynamic spectrum access for coexistence of 4G and future 5G systems," in *European Conference on Networks and Communications (EuCnC 2015)*, Paris, France, Jun. 2015.

[6] B. Zayen, F. Kaltenberger, and R. Knopp, *Opportunistic Spectrum Sharing and White Space Access: The Practical Reality*. Wiley, 2015, ch. OpenAirInterface and ExpressMIMO2 for spectrally agile communication.

[7] T. Yucek and H. Arslan, "A Survey of Spectrum Sensing Algorithms for Cognitive Radio Applications," *Communications Surveys Tutorials, IEEE*, vol. 11, no. 1, pp. 116–130, First 2009.

---

[1] http://www.openairinterface.org